

Influence of the Coulomb parameter U on partial densities of states of CuGeO_3 : comparison with X-ray spectral data

A.V. Galakhov^{1,a}, V.R. Galakhov¹, V.I. Anisimov¹, E.Z. Kurmaev¹, A.V. Sokolov¹, L. Gridneva², V.V. Maltsev³, L.I. Leonyuk³, A. Moewes⁴, S. Bartkowski⁵, M. Neumann⁵, and J. Nordgren⁶

¹ Institute of Metal Physics, Russian Academy of Sciences — Ural Division, 620219 Yekaterinburg GSP-170, Russia

² Department of Synchrotron Radiation Research, Institute of Physics, Lund University, Sölvegatan 14, 223 62 Lund, Sweden

³ Department of Crystallography, Faculty of Geology, Moscow State University, 119899 Moscow, Russia

⁴ Department of Physics and Engineering Physics, University of Saskatchewan, 116 Science Place, Saskatoon, Saskatchewan S7N 5E2, Canada

⁵ University of Osnabrück – Fachbereich Physik, 49069 Osnabrück, Germany

⁶ Department of Physics, Uppsala University, PO Box 530, 751 21 Uppsala, Sweden

Received 27 April 2004

Published online 21 October 2004 – © EDP Sciences, Società Italiana di Fisica, Springer-Verlag 2004

Abstract. The electronic structure of the strongly Coulomb correlated cuprate CuGeO_3 has been calculated by the local-density-approximation method (LDA+ U). The parameter U was varied from 0 to 8 eV. The results of the band-structure calculations are compared with experimental data obtained by means of X-ray photoelectron and resonant X-ray emission spectroscopy methods (Cu $L\alpha$ and O $K\alpha$ X-ray emission spectra). It is established that a LDA+ U calculation with $U = 4$ eV reproduces well the X-ray photoelectron and X-ray resonant emission spectral data.

PACS. 71.20.-b Electron density of states and band structure of crystalline solids – 78.70.En X-ray emission spectra and fluorescence – 79.60.-i Photoemission and photoelectron spectra

1 Introduction

CuGeO_3 is a layered compound with a spin-Peierls transition at ≈ 14 K [1] which implies the presence of strong electron-correlation effects. This transition is quite unusual for inorganic compounds. It can be viewed as a transition occurring along the Cu–O chains, from uniform antiferromagnetic spin- $\frac{1}{2}$ Heisenberg chains to a system of dimerized chains with a singlet ground state [2]. The assertion that the ground state is a spin singlet with a finite energy gap, which is responsible for the reduction of the magnetic susceptibility to zero for temperatures below 14 K [1], has been confirmed by inelastic neutron-scattering measurements [3].

Single crystals of CuGeO_3 are blue, clearly indicating their insulating nature. Transmission and absorption measurements with polarized light give gap values of ≈ 3.25 – 3.55 eV, depending on the polarization of the incoming light relative to the crystal axes [4,5].

Investigations of X-ray photoelectron spectra from the valence band and the core levels of CuGeO_3 were carried out by Terasaki et al. [6] and by Parmigiani et al. [7]. The Auger and Cu $2p \rightarrow 3d$ and Cu $3p \rightarrow 3d$ resonant photoemission spectra of CuGeO_3 were measured by Parmigiani

et al. [7]. It was shown that CuGeO_3 is a *charge-transfer* insulator with $\Delta \approx 4.2$ and $U_{dd} \approx 6.7$ eV [7]. CuGeO_3 is found to be more ionic than superconducting cuprates and than CuO [7]. Duda et al. [8] have carried out measurements of polarized resonant O $K\alpha$ spectra of CuGeO_3 and have observed a Zhang-Rice singlet.

Standard band-structure calculations using the LDA approach predict a metallic state for CuGeO_3 [9,10]. It is commonly accepted that the LDA usually gives a poor description of strongly correlated systems, as the on-site Coulomb interaction U of the localized d -electrons, that can be significant, is generally underestimated in LDA. The recently developed LDA+ U approach includes the leading terms for the on-site Coulomb and exchange interactions, U and J , allowing to obtain an insulating band-structure character in transition-metal oxides and in high-temperature superconductors [11]. Recently, the LDA+ U approach has been applied to band-structure calculations of CuGeO_3 in [12,13] with different d - d electron Coulomb and exchange-energy parameters, $U = 9.66$ eV and $J = 0.59$ eV in [12], or $U = 6.7$ eV and $J = 0.98$ eV in [13]. The calculations reproduce the insulating band structure of CuGeO_3 with band gaps of 3.02 eV [12] or 2.4 eV [13], and magnetic moments of $0.89 \mu_B$ [12] or $0.76 \mu_B$ [13].

^a e-mail: agalakhov@ifmlrs.uran.ru

However, the problem is to define the U -correction for LDA+ U calculations in an unambiguous manner. It is known that an overestimate of the screened Coulomb parameter U can lead to a large downward energy shift of the metal $3d$ states below the Fermi level [14,15]. This in turn leads to a poor agreement with the corresponding part of the observed spectra.

In the present paper, a combined study of the electronic structure of CuGeO₃ by X-ray emission and X-ray photoelectron spectroscopy is performed, which gives full information about the occupied partial and total density of states distributions, respectively. It is shown that these spectra can be directly compared with available and specially performed LDA and LDA+ U calculations of CuGeO₃ and used as experimental criterion to determine the U parameter.

2 Calculation

The band structure calculation of CuGeO₃ was performed with the LDA+ U approach [11]. We used a self-consistent linearized muffin-tin orbital (LMTO) method within this approximation. To show the approach [11] we employed a self-consistent tight-binding linearized muffin-tin orbital (TB-LMTO) method using the atomic sphere approach (ASA) within this approximation. To find the dependence of the calculated electronic structure on the Coulomb parameter U , a set of fixed values of U was taken instead of the calculated one. According to [12], U takes the large value 9.66 eV, obtained from the constrained density-functional calculation. Thus, we used a wide range of U -values from zero (pure LDA) to 8 eV in 2 eV steps. The exchange-parameter J was held constant at 1 eV in all calculations except for the LDA one, in which it was equal to zero. We know from our own experience that the value of J only has a relatively small influence on the results of these calculations, as opposed to the effect of U .

3 Experimental details

A single crystal of CuGeO₃ was grown by the self-flux method. Appropriate growth conditions were determined on the basis of the analysis of microstructure and physical properties. The crystal structure of the sample was checked by X-ray structural analysis with a DRON-3 diffractometer.

X-ray photoelectron spectra were measured using an ESCA spectrometer from Physical Electronics (PHI 5600 ci) with monochromatic Al $K\alpha$ radiation. The energy resolution was approximately 0.4 eV. The pressure in the vacuum chamber during the measurements was below 5×10^{-9} mbar. The spectrometer was calibrated using the Au $4f_{7/2}$ signal from an Au-foil [$E_B(4f_{7/2}) = 84.0$ eV]. The single-crystal specimen of CuGeO₃ was cleaved in situ. Since the sample is an insulator, a charging effect occurred. The spectra were corrected for this charging using the Ge $2p_{3/2}$ core line (with a binding energy of 1219.5 eV [7]).

The Cu $L\alpha, \beta$ X-ray emission spectra ($3d \rightarrow 2p_{3/2,1/2}$ transition) were measured at the Advanced Light Source of the Ernest Orlando Lawrence Berkeley National Laboratory, on beamline 8.0. The fluorescent radiation emitted by the sample was analyzed with a high-resolution grating spectrometer computer-interfaced to a multi-channel detector. The pressure in the sample chamber was below 10^{-8} mbar during the measurements. The Cu $L\alpha, \beta$ X-ray emission spectra were recorded with an 10 m radius, 1500 lines/mm grating. The spectrometer resolution was about 2.5 eV.

The O $K\alpha$ X-ray emission spectra ($2p \rightarrow 1s$ transition) were measured on the bulk branch line of beamline I511 at MAX II (MAX-lab National Laboratory, Sweden). The spectra were obtained using a high-resolution Rowland-mount grazing-incidence grating spectrometer with a two-dimensional detector [16]. The energy scale was calibrated using the Zn $L\alpha$ and $L\beta$ spectra in second order of diffraction from the spectrometer grating.

The X-ray emission spectra were brought to the scale of the binding energies with respect to the Fermi level using the binding energies of the O $1s$ and Cu $2p$ initial (core-level) states of the X-ray transitions as measured by XPS.

4 Results and discussion

Cu $3d$ and O $2p$ partial densities of states of CuGeO₃ calculated within the LDA+ U scheme with $U = 0, 2, 4, 6,$ and 8 eV are presented in Figure 1. One sees that, together with the increase of U from 0 to 8 eV, a gap opens up between the occupied and unoccupied states. The maximal value of this gap, which is 1.58 eV, is obtained for $U = 8$ eV. This maximum gap is below the experimental value (≈ 3.25 – 3.55 eV [4,5]). As the parameter U increases, O $2p$ states move to higher energies (closer to the Fermi level) but the Cu $3d$ ones shift toward lower energies.

Information about the Cu $3d$ partial distribution in the valence state can be obtained using Cu $L\alpha$ X-ray emission spectra. Cu $L\alpha, \beta$ X-ray emission spectra originate from Cu $3d \rightarrow 2p$ electron transitions. Cu $L\alpha$ X-ray emission spectra excited with high energy electrons or photons show a satellite on the high-energy side of the main peak. This satellite originates from the decay of L_2 core holes in the presence of additional $3d$ vacancies. In order to avoid this satellite, the spectra should be excited at lower energies than the L_2 ($2p_{1/2}$) ionization threshold.

In Figure 2 we present the measurements of Cu $L\alpha, \beta$ X-ray emission spectra of CuGeO₃ for selected photon energies. The excitation energy was tuned from 927 to 971 eV, which includes the Cu L_3 and Cu L_2 absorption thresholds. The excitation energies are labelled by arrows. At lower exciting photon energies (up to 936 eV), the Cu $L\alpha$ line is distorted by elastic peaks whose energies coincide with the excitation energies. The best approximation for valence $3d$ states is given by the spectrum obtained at an exciting photon energy of about 945 eV. This spectrum is not distorted by the satellite

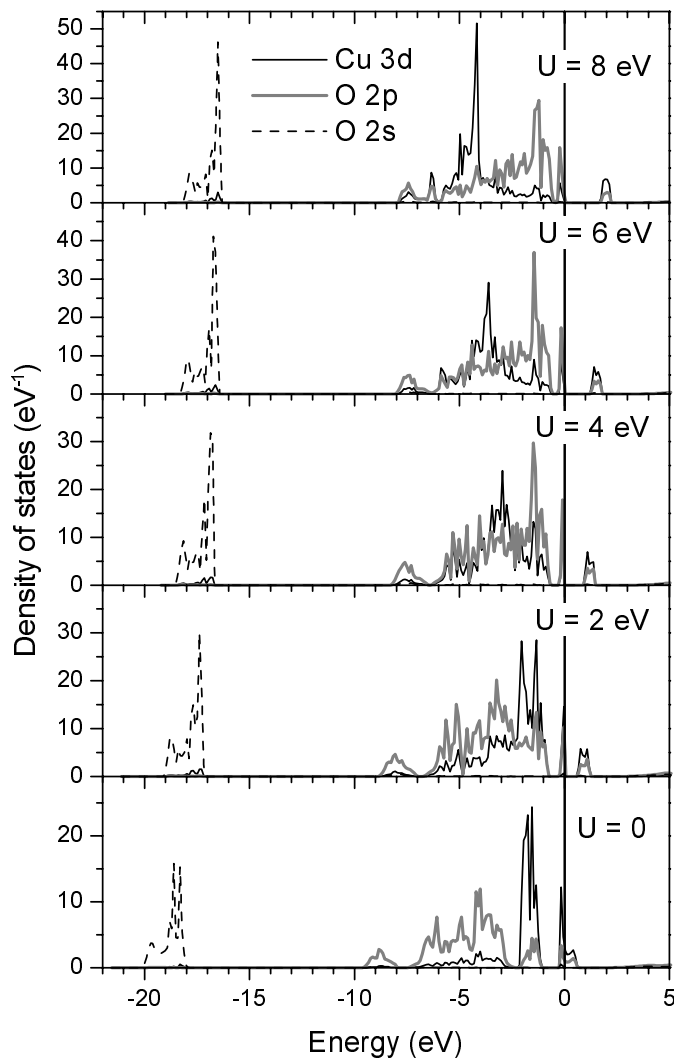


Fig. 1. Cu 3d (solid line), O 2p (shaded area), and O 2s (broken line) partial densities of states of CuGeO_3 calculated using the LSDA+ U approximation for $U = 0, 2, 4, 6,$ and 8 eV.

and has a rather high intensity. The Cu $L\alpha$ spectra measured at excitation energies of 950.5 eV and 971.0 eV have satellites at about 934 eV.

O 2p states are represented by O $K\alpha$ X-ray emission spectra (O 2p \rightarrow 1s transition). These spectra of CuGeO_3 measured at excitation energies of 531.7–535.3 eV are shown in Figure 3. The spectra are in good agreement with those measured by Duda et al. [8] with the polarization vector of the incoming X-ray beam parallel to the a axis.

The vertical bars in the O 1s X-ray absorption spectrum mark the incident photon energies. The excitation energies (from 531.7 eV to 535.3 eV) for the emission spectra are shown by the solid inclined line.

O $K\alpha$ resonant X-ray emission spectra of CuGeO_3 can be explained in terms of both band-like states (main emission band) and localized excitonic states (inelastic scattering) [8]. According to Okada and Kotani [17,18], both the Zhang-Rice singlet (ZR) and dd excitations are character-

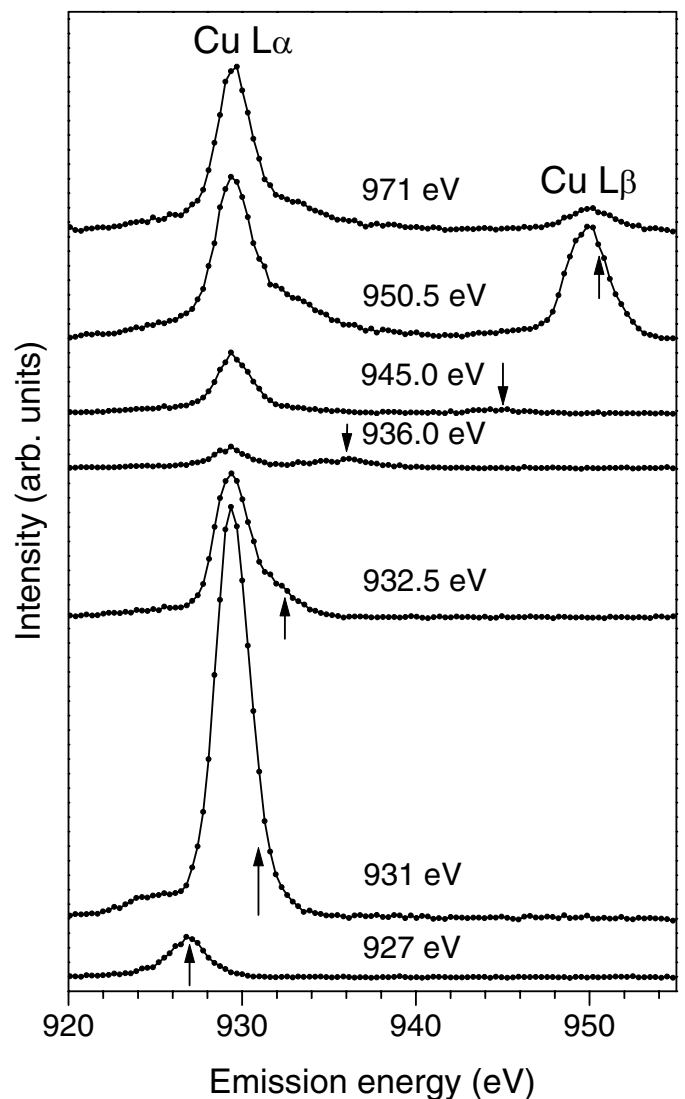


Fig. 2. Excitation-energy dependence of Cu $L\alpha, \beta$ X-ray emission spectra of CuGeO_3 measured at excitation energies of 927–971 eV. Arrows indicate the excitation energies.

ized by a Raman shift of 2–4 eV. The energy positions of these peaks in the emission energy scale are shown by the slanted line. This position is constant in the Raman-shift scale and depends on the excitation energy in the emission-energy scale. The region of the d^8 states at lower emission-energy scale is also marked by an oblique line [17,18].

The shaded area shows the band-like part of the spectra. According to the soft O 1s X-ray absorption study of CuGeO_3 [19] and the calculations of O 2p empty density of states using a multiband Hubbard Hamiltonian [20], unoccupied O 2p states of in-plane oxygen atoms (O2) are located at the bottom of the empty part of the valence band (peak a at the O 1s X-ray absorption spectrum presented in Fig. 3). This means that the O $K\alpha$ emission spectrum excited at 532.6 eV (which corresponds to peak a of the O 1s X-ray absorption spectrum) reveals mainly 2p states of in-plane oxygen atoms. Peak b (534.0 eV) of the O 1s X-ray absorption spectrum corresponds to

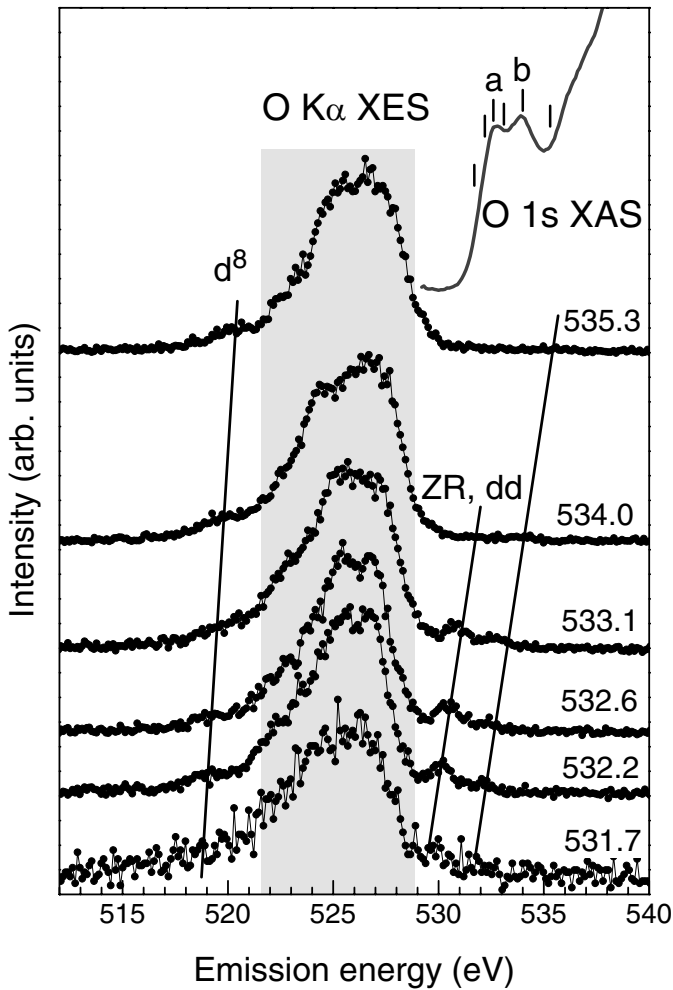


Fig. 3. O 1s X-ray absorption (XAS) and O K α (XES) resonant X-ray emission spectra of CuGeO₃. X-ray emission spectra are measured at excitation energies of 531.7–535.3 eV shown by a slanted line. ZR and *dd* denote Zhang-Rice singlet and *dd* excitations, respectively. *d*⁸ denotes the *d*⁸ final state configuration. The shaded area shows the band-like part of the spectra.

a superposition of 2*p* states from both apical (O1) and in-plane oxygen atoms (O2). This means that the spectrum excited at 534 eV is produced from both sites with different weights. The main contribution to this spectrum arises from in-plane oxygen atoms (O2).

Our X-ray photoelectron data obtained for CuGeO₃ agree well with those obtained by Parmigiani et al. [7]. Figure 4 shows the Cu 2*p* photoelectron spectrum of CuGeO₃. In addition to the main lines at 934.7 and 954.7 eV, broad satellites, as expected for the Cu²⁺ cuprates, appear in the binding-energy ranges of 939–945 eV and 960–964 eV for the Cu 2*p*_{3/2} and Cu 2*p*_{1/2} lines, respectively. The satellites show a fine structure, whose origin in cuprates is widely described in the literature [21], arising from multiplet-splitting effects owing to the interaction between the 2*p* core hole and the 3*d*⁹ electronic configuration in the final state of the photoemission process.

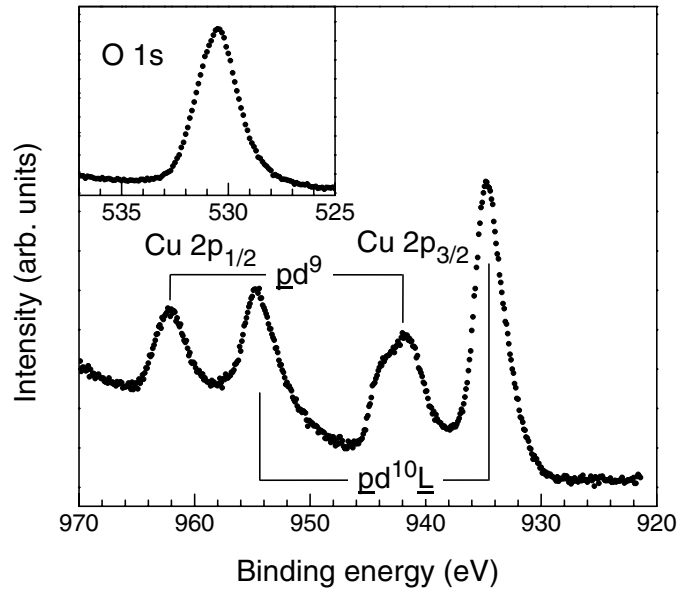


Fig. 4. Cu 2*p*_{3/2,1/2} and O 1s (in inset) X-ray photoelectron spectra of CuGeO₃.

The main peaks are described mainly by $\underline{pd}^{10}\underline{L}$ states, while the satellite structure should be primarily due to \underline{pd}^9 states. Here, \underline{L} denotes a ligand hole arising after the transfer of an electron from a 2*p* ligand level to a metal 3*d* level and \underline{p} is a metal 2*p* hole in the final state of the photoemission process.

The inset in Figure 4 presents the O 1s X-ray photoelectron spectrum of CuGeO₃. Although the crystal structure of CuGeO₃ is characterized by two nonequivalent oxygen atoms, the O 1s X-ray photoelectron spectrum of CuGeO₃ shows only one line. It follows that both in-plane oxygen atoms (O2) and apical oxygen atoms (O1) have equal O 1s binding energies, which according to our experiments are equal to 530.5 eV.

Figure 5 shows the valence-band X-ray photoemission spectrum and the Cu L α and O K α X-ray emission spectra of CuGeO₃. The X-ray emission spectra are arranged with respect to the Fermi level, taking into account the Cu 2*p*_{3/2} ($E_B = 934.7$ eV) and O 1s ($E_B = 530.5$ eV) core-level binding energies measured by X-ray photoelectron spectroscopy.

For the Al K α excitation, photoelectron cross-sections σ multiplied by the atomic concentrations c , $\sigma(\text{Cu}3d)c(\text{Cu}) : \sigma(\text{Ge}4p)c(\text{Ge}) : \sigma(\text{O}2p)c(\text{O})$, are equal to 1 : 0.06 : 0.06 [22]. In consequence, the valence-band X-ray photoelectron spectrum results mainly from Cu 3*d* states. Based on the analysis of the X-ray photoelectron spectrum of CuGeO₃ done by Parmigiani et al. [7], peak *A* is assigned to $d^9\underline{L}$ final states, while components *B* and *C* could be assigned to *d*⁸ states with a smaller contribution of $d^{10}\underline{L}^2$ states. Here, \underline{L} denotes a ligand hole arising after the transfer of an electron from a 2*p* oxygen level to a copper 3*d* level, and \underline{L}^2 denotes two holes in a 2*p* oxygen level owing to the charge-transfer process. According to the configuration-interaction calculations [23], the shoulder *D* in the photoelectron spectrum of CuO has the sym-

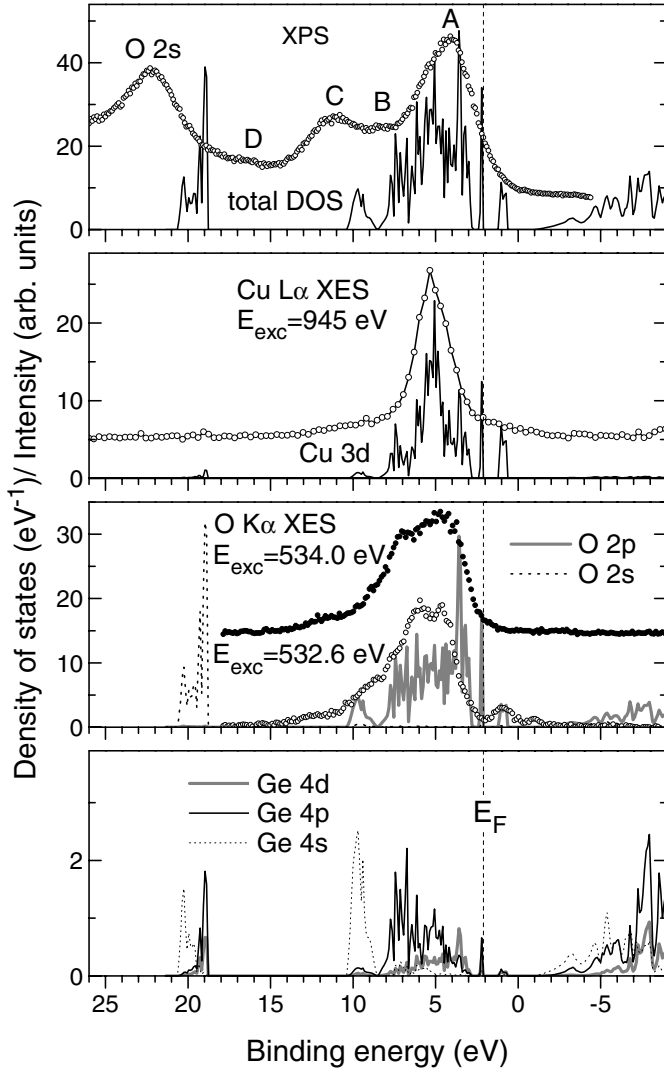


Fig. 5. X-ray photoelectron spectrum of the valence band and $\text{Cu L}\alpha$ and $\text{O K}\alpha$ X-ray emission spectra of CuGeO_3 compared with total and partial densities of states calculated using the $\text{LSDA}+U$ approximation for $U = 4$ eV. X-ray emission spectra are brought to a common energy scale using the core-level electron binding energies. The $\text{Cu L}\alpha$ emission spectrum was measured at the excitation energy of 945 eV. The $\text{O K}\alpha$ emission spectra were measured at the excitation energies of 532.6 eV and 534.0 eV.

metry of a singlet 1A_1 derived from the free-atom 1S state. This interpretation is confirmed by resonant $\text{Cu } 2p \rightarrow 3d$ photoemission experiments [7]. We can compare the structure A ($d^9\bar{L}$ final-state configuration) with results of the band-structure calculations.

The $\text{Cu L}\alpha$ spectrum coincides with the $\text{O K}\alpha$ spectrum. It indicates a strong $\text{O } 2p$ – $\text{Cu } 3d$ hybridization. According to the LDA calculation done without the correlation correction, $\text{Cu } 3d$ states are located near the Fermi level, and $\text{O } 2p$ states are found in a region from -3 to -7 eV (see Fig. 1). For the $\text{LSDA}+U$ calculation with $U = 8$ eV, the relative positions of $\text{O } 2p$ and $\text{Cu } 3d$ states are changed: $\text{O } 2p$ states are located near the Fermi

level while the maximum of the $\text{Cu } 3d$ distribution is at about -4.5 eV.

We have compared the total and partial densities of states obtained for $U = 4$ eV with X-ray photoelectron and X-ray emission spectra in Figure 5. The calculated data are shifted by 2.15 eV with respect to the measured ones. This shift is necessary because CuGeO_3 is an insulator and therefore it is expected that the calculated (top of the valence band) and the experimental (in the gap) Fermi energies do not coincide (see, for example, [24]).

The relative position of $\text{O } 2p$ and $\text{Cu } 3d$ states are best described by an $\text{LSDA}+U$ calculation with a Coulomb energy $U = 4$ eV. However, the energy gap seems smaller than the experimental one in all these calculations, even at $U = 8$ eV. It might reach the correct value for U larger than 8 eV, however the position of the states will then be totally wrong. It cannot be excluded that the experimentally observed gap is not produced by the small peak in the density of states which is calculated near 1.5 eV. This peak is isolated from the rest of the conduction band which starts at about twice that energy. If the latter produces the experimental gap, then the agreement of our calculation with all experiments would be quite good indeed.

5 Conclusion

In summary, we present X-ray photoelectron and soft $\text{Cu L}\alpha$ and $\text{O K}\alpha$ X-ray resonant emission spectra of CuGeO_3 . The $\text{Cu L}\alpha$ spectrum overlaps on the binding energy scale with the $\text{O K}\alpha$ spectrum indicating strong $\text{O } 2p$ – $\text{Cu } 3d$ hybridization. From comparison of experiment and calculation, we conclude that the $\text{LSDA}+U$ calculation with $U = 4$ eV best reproduces the X-ray photoelectron and resonant emission spectra.

This work was supported by the Russian Foundation for Basic Research (Grant No 04-03-96092-Ural), the Research Council of the President of the Russian Federation (Project NSH-1026.2003.2), the Russian Ministry for Industry and Science (Project on Superconductivity of Mesoscopic and Strongly Correlated Systems), the grants “Cooperation between the Royal Swedish Academy of Sciences and Former Soviet Union States”, the Natural Sciences and Engineering Research Council of Canada (NSERC), and NATO Collaborative Linkage Grant (PST.CLG.978044) which are gratefully acknowledged. One of the authors (V. R. G.) gratefully acknowledges fellowship support from the Deutscher Akademischer Austauschdienst (DAAD) Program.

References

1. H. Masashi, T. Ichiro, U. Kunimitsu, *Phys. Rev. Lett.* **70**, 3651 (1993)
2. H. Takahashi, N. Mori, O. Fujita, J. Akimitsu, T. Matsumoto, *Solid State Commun.* **95**, 817 (1985)
3. M. Nishi, O. Fujita, J. Akimitsu, *Phys. Rev. B* **50**, 16508 (1994)
4. S.D. Dević, Ph.D. thesis, University of Belgrade, 1996

5. M. Bassi, P. Camagni, R. Rolli, G. Samoggia, F. Parmigiani, G. Dhalène, A. Revcolevschi, *Phys. Rev. B* **54**, R11030 (1996)
6. I. Terasaki, R. Itti, N. Koshizuka, M. Hase, I. Tsukada, K. Uchinokura, *Phys. Rev. B* **52**, 295 (1995)
7. F. Parmigiani, L. Sangaletti, A. Goldoni, U. del Pennini, C. Kim, Z.-X. Shen, A. Revcolevschi, G. Dhalène, *Phys. Rev. B* **55**, 1459 (1997)
8. L.-C. Duda, J. Downes, C. McGuinness, T. Schmitt, A. Augustsson, K.E. Smith, G. Dhalène, A. Revcolevschi, *Phys. Rev. B* **61**, 4186 (2000)
9. L.F. Mattheiss, *Phys. Rev. B* **49**, 14050 (1994)
10. Z.V. Popović, S.D. Dević, V.N. Popov, G. Dhalène, A. Revcolevschi, *Phys. Rev. B* **52**, 4185 (1995)
11. V.I. Anisimov, J. Zaanen, J.W. Allen, *Phys. Rev. B* **44**, 943 (1991)
12. Ž.V. Šljivančanin, Z.S. Popović, F.R., Vukajlović, *Phys. Rev. B* **56**, 4432 (1997)
13. Hua Wu, Mei-chun Qian, Qing-qi Zheng, *J. Phys. Condens.: Matter* **11**, 209 (1999)
14. V.R. Galakhov, A.I. Poteryaev, E.Z. Kurmaev, V.I. Anisimov, S. Bartkowski, M. Neumann, Z.W. Lu, B.M. Klein, T.R. Zhao, *Phys. Rev. B* **56**, 4584 (1997)
15. D.A. Zatsepin, V.R. Galakhov, M.A. Korotin, V.V. Fedorenko, E.Z. Kurmaev, S. Bartkowski, M. Neumann, R. Berger, *Phys. Rev. B* **57**, 4377 (1998)
16. J. Nordgren, G. Bray, S. Cramm, R. Nyholm, J.-E. Rubensson, N. Wassdahl, *Rev. Sci. Instrum.* **60**, 1690 (1989)
17. K. Okada, A. Kotani, *Phys. Rev. B* **63**, 045103 (2001)
18. K. Okada, A. Kotani, *Phys. Rev. B* **65**, 144530 (2002)
19. V. Corradini, A. Goldoni, F. Parmigiani, C. Kim, A. Revcolevschi, L. Sangaletti, U. del Pennino, *Surf. Sci.* **420**, 142 (1999)
20. A. Villaforita, F. Manghi, F. Parmigiani, C. Calandra, *Solid State Commun.* **104**, 301 (1997)
21. G. van der Laan, C. Westra, C. Haas, G.A. Sawatzky, *Phys. Rev. B* **23**, 4369 (1981)
22. J.J. Yeh, I. Lindau, *Atomic Data and Nucl. Data Tables* **32**, 1 (1985)
23. H. Eskes, G.A. Sawatzky, *Phys. Rev. Lett.* **61**, 1415 (1988)
24. S. Hüfner, *Photoelectron Spectroscopy* (Springer, Heidelberg, 1995), p. 209